

Spectroscopic properties of lead fluoroborate glasses codoped with Er^{3+} and Yb^{3+}

Luciana Reyes Pires Kassab, Lilia Coronato Courrol, Alessandro Santos Morais, and Sonia Hatsue Tatumi

Faculdade de Tecnologia de São Paulo, Centro Estadual de Educação Tecnológica Paula Souza, Praça Coronel Fernando Prestes 30, CEP 01124-060, São Paulo, São Paulo, Brazil

Niklaus Ursus Wetter and Laércio Gomes

Centro de Lasers e Aplicações, IPEN-SP, Travessa R 400, Cidade Universitária, CEP 05508-900, São Paulo, São Paulo, Brazil

Received March 25, 2002; revised manuscript received July 15, 2002

Energy transfer at 1500 nm in lead fluoroborate glasses ($\text{PbO-PbF}_2\text{-B}_2\text{O}_3$) codoped with Er^{3+} and Yb^{3+} is studied for the first time to the authors' knowledge. A sample codoped with 1 mol. % of Yb_2O_3 and 0.01 mol. % of Er_2O_3 has a measured fluorescence lifetime of (1.30 ± 0.07) ms and an energy transfer efficiency of 80%. Also, a large emission band, of 72.4 nm has a measured peak emission cross section of $(0.73 \pm 0.06) \times 10^{-20}$ cm^2 . The calculated Judd-Ofelt parameters are $\Omega_2 = (3.51 \pm 0.14) \times 10^{-20}$ cm^2 , $\Omega_4 = (1.09 \pm 0.07) \times 10^{-20}$ cm^2 , and $\Omega_6 = (0.94 \pm 0.07) \times 10^{-20}$ cm^2 . The temporal evolution of the Yb^{3+} fluorescence is fitted by use of the Yokota-Tanimoto expression to yield the Yb^{3+} diffusion constant [$(1.6 \pm 0.2) \times 10^{-10}$ $\text{cm}^2 \text{s}^{-1}$] and the critical radius of $\text{Yb}^{3+}/\text{Er}^{3+}$ $(18 \pm 1) \times 10^{-8}$ cm. Results with the singly doped samples produced are presented to clarify the energy transfer process. © 2002 Optical Society of America
OCIS codes: 160.2750, 160.4760, 160.5690, 160.3380, 140.3380.

1. INTRODUCTION

Spectroscopic properties of erbium ions in several glass hosts have been the subject of extensive investigations. Since the first operation of the erbium laser in the pulsed regime in 1965,¹ the erbium glass laser has been attracting much interest, mainly because of its emission wavelength (1530 nm), which is located in the eye-safe region,² and its applications for telecommunications. More recently, with the development of strained-layer InGaAs laser diodes emitting at the 980-nm pump wavelength,³ laser physicists have given much attention to continuous-wave laser oscillators based on Er^{3+} -doped glasses and optical fibers. This interest was also stimulated by the successful operation of an erbium-doped fiber amplifier pumped at 980 nm,⁴ which rapidly turned out to be a key component in all modern optical transmission systems. Erbium ions, when they are hosted in a glass material, exhibit a broad emission band located near 1.5 μm . This large emission spectrum is mainly homogeneously broadened, and it can be used to obtain quasi-three-level laser action at this wavelength. The Yb^{3+} ion can be an excellent sensitizer for Er^{3+} , and the main advantage of using it as a codopant is that it will improve the pumping efficiency while strongly reducing the laser threshold. The use of erbium-doped glasses codoped with ytterbium is an effective way to enhance absorption and pumping efficiencies, particularly for short cavity length devices (bulk microlasers or certain fiber lasers).⁴ The process of energy transfer between Yb^{3+} and Er^{3+} ions in the codoped active material substantially reduces the intensity of noise

induced by pump-power fluctuations.⁵ The Yb^{3+} 4*f* electron configuration has a small number of well-spaced 4*f* states; the probability of energy loss through interstate nonradiative transitions is therefore smaller than that observed in other rare-earth ions. Besides, materials doped with Yb^{3+} ions are more efficient emitters when they are pumped by diode lasers, without the possibility of excited-state absorption. They are also of interest for the next generation of high-intensity lasers because of their energy storage properties.⁶

We present, for the first time to our knowledge, results of energy transfer in fluoroborate glasses codoped with erbium and ytterbium. Results for samples singly doped with Yb^{3+} and Er^{3+} are also shown to explain the energy transfer. The spectroscopic properties are determined by means of optical absorption, luminescence, and associated lifetime. Also, calculations of the Judd-Ofelt parameters, probability of spontaneous emission, and emission cross sections are derived. The decay rate of the donor ion Yb^{3+} is described by use of the Yokota-Tanimoto model.

The properties of this new glass matrix that have stimulated our study are its high refractive index (2.2), which is normally responsible for the high probability of spontaneous emission, its good glass-forming region, its good physical and chemical stability, and its transmission from the visible region (0.4 μm) to the long infrared (4 μm).⁷

The most important Er^{3+} ion laser transitions are found in the infrared. One of them is at 2700 nm (with

interest in the domain of optical sources for sensors and for medicine), where the fundamental stretching vibration of OH^- takes place. The efficiency of this emission in oxide glasses is low because the ${}^4I_{11/2} \rightarrow {}^4I_{13/2}$ transition, which responsible for this emission, suffers strong nonradiative, multiphonon relaxation. Glasses with reduced phonon energy can enhance the quantum efficiency of the 2700-nm emission, as occurs with sulfide and heavy metal oxide glass hosts. Another important emission of Er^{3+} ions occurs at 1500 nm, which coincides with the third optical communication window. This is the transition that provides amplification near 1540 nm in erbium-doped fiber amplifiers and eye-safe radiation for remote-sensing applications. Codoping with ytterbium is also a convenient way to obtain laser emission at this wavelength because of the wide applications of ytterbium in optoelectronic circuits. Yb^{3+} as a codopant in an Er^{3+} -doped laser host is interesting because of its broad absorption band and its high absorption cross section near 970 nm.

We have studied the 1500-nm emission of Er^{3+} in singly and codoped fluoroborate glasses to determine the effect of ytterbium as a sensitizer in this host. We remark that the results of studies of lead fluoroborate glasses singly doped with various concentrations of Yb^{3+} were previously published.^{7,8}

2. EXPERIMENT

The samples (singly doped with Er_2O_3 or Yb_2O_3 and codoped with both of them) were prepared with the following glass matrix⁸ [mol. %]: $43.5\text{H}_3\text{BO}_3$ – 22.5PbCO_3 – 34.0PbF_2 . The appropriate mixture of reagents was melted in air at 1000 °C for 1.5 h in a platinum crucible and then poured into a preheated brass mold to be annealed for 12 h at 400 °C (the measured glass-transition temperature, T_g , is 480 °C). Transparent and homogeneous glasses (all samples were examined by optical microscopy) that were stable against crystallization were produced, cut into slabs of 3-mm thickness, and then polished for optical measurements. The refractive index (2.20 ± 0.03) was measured by the apparent-depth method (which relates the physical thickness to the optical thickness or the apparent thickness of the refractive index), and the density (4.4 ± 0.1) g/cm³ was determined with the Archimedes method. Absorption spectra (with an error of $\pm 2\%$) at room temperature were obtained with a spectrophotometer (Cary 17 D/OLIS). The luminescence spectra were determined by use of an excitation beam from an InGaAs laser diode (Optopower A020) at 968 nm, a 0.5-m Spex monochromator, a germanium detector, and an EG&G 7220 lock-in amplifier. The trivalent ions had their lifetimes measured by pulsed laser excitation (4 ns) from an optical parametric oscillator pumped by a frequency-doubled Nd:YAG laser (Quantel) with a fast S-20 extended-type photomultiplier and analyzed with a signal-processing boxcar averager (PAR 4402). To avoid reabsorption effects in the emission and lifetime measurements, we placed the sample such that the laser beam passed close to the sample's edge. The luminescence emitted from this edge was collected and used for the measurements. Besides, the sample was placed

in an experimental setup in which the pump and the emission beams were perpendicular.

3. RESULTS

The process of energy transfer between Yb^{3+} and Er^{3+} is schematized in Fig. 1. Arrows (a) and (b) indicate radiative absorption and emission of a pump photon from the ${}^2F_{7/2}$ and ${}^2F_{5/2}$ ytterbium levels, respectively, (c) is the spontaneous decay from the ${}^2F_{5/2}$ ytterbium level, (d) is the ytterbium-to-erbium energy transfer process, which acts as indirect pumping of erbium ions, (e) is the erbium nonradiative decay from the ${}^4I_{11/2}$ level to the ${}^4I_{13/2}$ upper laser level, (f) and (g) are the stimulated emission and absorption, respectively, between the ${}^4I_{13/2}$ erbium laser level and the $I_{15/2}$ ground level, (h) is the erbium spontaneous decay from $I_{13/2}$ level, and (i) is a cooperative upconversion process between two excited erbium ions that promotes one ion to the $I_{9/2}$ upper level while the second ion decays to the ground level. The first ion then relaxes, through fast nonradiative decay, to its original ${}^4I_{13/2}$ state such that the overall effect is the loss of one excited ion, ${}^4I_{13/2}$. Note that a uniform upconversion can be assumed.⁹

Absorption measurements performed at room temperature show peaks that are associated with the electronic transitions of Er^{3+} (521, 545, 652, 797, 968, and 1532 nm) and of Yb^{3+} (968 nm) and are a proof of the incorporation of the rare-earth ions in trivalent form.

The Yb^{3+} emission spectra at 1022 nm (Fig. 2), for the samples singly doped with 1 mol. % of Yb_2O_3 and codoped with Yb_2O_3 (1 mol. %) and Er_2O_3 (0.01 mol. %) are obtained by excitation at 968 nm. The emission of Yb^{3+} is significantly decreased for the codoped sample, showing the role of Yb^{3+} as sensitizer.

The absorption cross-section spectrum of the sample, singly doped with 1 mol. % of Yb_2O_3 , is shown in Fig. 3. Notice the high absorption cross section of $(2.80 \pm 0.19) \times 10^{-20}$ cm² at 968 nm, which is related to the ${}^2F_{7/2} \rightarrow {}^2F_{5/2}$ transition of Yb^{3+} .

The Er^{3+} emission spectra at 1543 nm, related to the ${}^4I_{13/2} \rightarrow {}^4I_{15/2}$ transition (Fig. 4) for the samples singly doped with Er_2O_3 (0.2 and 1 mol. %) and codoped with Yb_2O_3 (1 mol. %) and Er_2O_3 (0.01 mol. %), are obtained by excitation at 968 nm. The erbium emission of the codoped sample is enhanced compared with those of the singly doped samples because of the action of Yb^{3+} as sensitizer. Quenching can be observed for concentrations of Er_2O_3 higher than 2 mol. %. The emission cross-section spectrum of Er^{3+} in the codoped sample is shown in Fig.

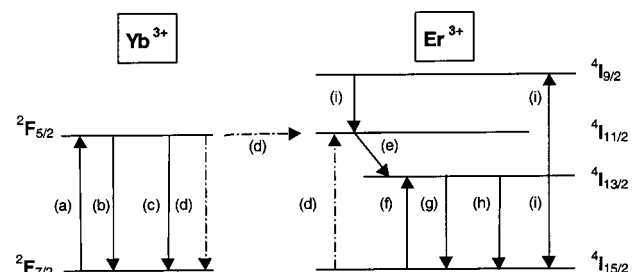


Fig. 1. Energy transfer between Yb^{3+} and Er^{3+} .

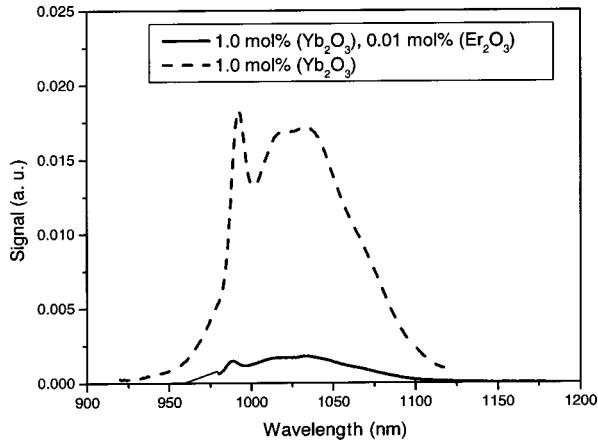


Fig. 2. Emission spectra of Yb^{3+} for the lead fluoroborate glass (excitation at 968 nm).

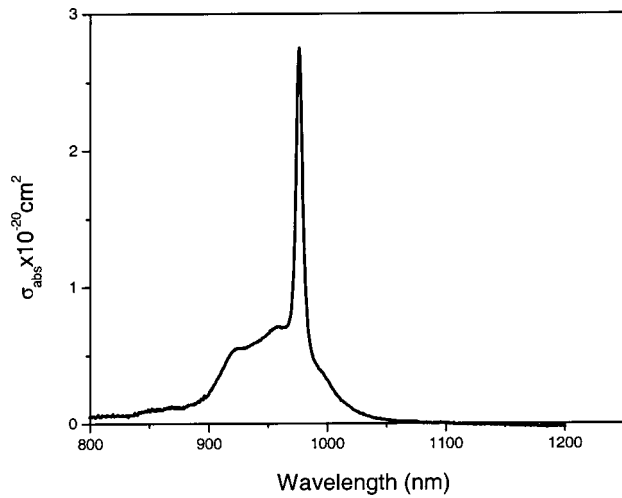


Fig. 3. Absorption cross-section spectrum of Yb^{3+} for the lead fluoroborate glass that has been singly doped with 1 mol. % of Yb_2O_3 .

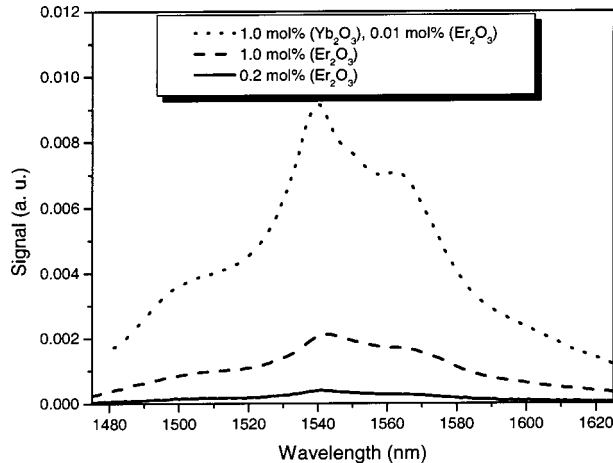


Fig. 4. Emission spectra of Er^{3+} for the lead fluoroborate glass, related to the ${}^4I_{13/2} \rightarrow {}^4I_{15/2}$ transition (excitation at 968 nm).

5. The peak emission cross section is $(0.73 \pm 0.06) \times 10^{-20} \text{ cm}^2$ at 1543 nm. We calculated this emission cross section, using the Judd–Ofelt parameters and the probability of spontaneous emission, as explained below.^{10,11}

The Judd–Ofelt parameters (Ω_t) were calculated with the following expression [with the six absorption bands of the electronic transitions of Er^{3+} from the initial manifold (S, L, J) to the final manifold (S', L', J')], which equates the experimental to the calculated oscillator strength for induced electric and magnetic dipole transitions:

$$\frac{mc^2}{\pi e^2 \rho \lambda_p^2} \int k(\lambda) d\lambda = \frac{8\pi^2 mc}{3h(2J+1)\lambda_p} \left[\frac{(n^2+2)^2 S_{\text{ed}}}{9n} + n S_{\text{md}} \right], \quad (1)$$

where c represents the velocity of light, n is the refractive index, ρ is the concentration of Er^{3+} ions, λ_p is the absorption peak wavelength, e and m are the mass and the electron charge, respectively, $k(\lambda)$ is the absorption coefficient, and S_{ed} and S_{md} are the line strengths for the induced electric and magnetic dipole transitions respectively. The line strength for the induced electric dipole (S_{ed}) transition is given by

$$S_{\text{ed}} = \sum_{t=2,4,6} \Omega_t |\langle SLJ || U^t || S'L'J' \rangle|^2, \quad (2)$$

where $|\langle SLJ || U^t || S'L'J' \rangle|^2$ is the square of the matrix elements of tensorial operator U^t , which connects the SLJ and the $S'L'J'$ states (determined from the literature).¹²

Because the magnetic dipole oscillator strength of the ${}^4I_{15/2} \rightarrow {}^4I_{13/2}$ transition exerts a considerable effect on the total radiative transition, it has to be considered in the calculation of the Judd–Ofelt parameters.

In Eq. (1) the oscillator strength for the magnetic dipole transition is given by

$$f_{\text{md}} = \frac{8\pi^2 mc S_{\text{md}} n}{3h(2J+1)\lambda_p} = f' n,$$

where $f' = 30.8 \times 10^{-8}$ for the ${}^4I_{15/2} \rightarrow {}^4I_{13/2}$ transition of Er^{3+} .¹¹ For $n = 2.2$, f_{md} has a value of 67.8×10^{-8} . The three Judd–Ofelt parameters are determined by a least-squares fitting routine that compares the measured oscillator strengths for the six different

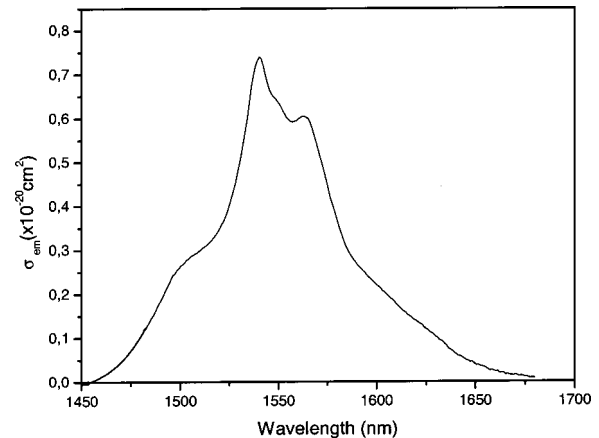


Fig. 5. Emission cross-section spectrum of Er^{3+} , related to the ${}^4I_{13/2} \rightarrow {}^4I_{15/2}$ transition, for lead fluoroborate glass codoped with Yb_2O_3 (1 mol. %) and Er_2O_3 (0.01 mol. %).

Er^{3+} absorption bands with the theoretical oscillator strengths, using the matrix elements tabulated in Ref. 12. The values obtained are

$$\Omega_2 = (3.51 \pm 0.14) \times 10^{-20} \text{ cm}^2,$$

$$\Omega_4 = (1.09 \pm 0.07) \times 10^{-20} \text{ cm}^2,$$

$$\Omega_6 = (0.94 \pm 0.07) \times 10^{-20} \text{ cm}^2.$$

The probability of spontaneous emission of 340.6 s^{-1} , from the initial manifold ($S, L, J = 13/2$) to the final manifold ($S', L', J' = 15/2$), was determined with the following equation¹⁰:

$$A_R = \frac{64\pi^4 e^2}{3h(2J+1)\lambda^3} \left[\frac{n(n^2+2)^2 S_{\text{ed}}}{9} + n^3 S_{\text{md}} \right]. \quad (3)$$

In Eq. (3), λ is the emission peak wavelength.

The peak emission cross section for the $\text{Er}^{3+} \ ^4I_{13/2} \rightarrow \ ^4I_{15/2}$ transition is expressed as

$$\sigma_{\text{em}} = \frac{\lambda^4 A_R}{8\pi n^2 c \Delta\lambda_{\text{EFF}}}, \quad (4)$$

where $\Delta\lambda_{\text{EFF}}$ is the effective fluorescence bandwidth (72.4 nm).

The fluorescence lifetimes measured were fitted with a single exponential function, and the results are shown in Table 1. The emission lifetime, obtained for the $\ ^4I_{13/2} \rightarrow \ ^4I_{15/2}$ transition of Er^{3+} , decreased from $(1.30 \pm 0.07) \text{ ms}$ (0.2 mol. %) to $(0.80 \pm 0.04) \text{ ms}$ (2 mol. %). The same transition has a lifetime of $(1.30 \pm 0.07) \text{ ms}$ in the codoped sample. For the singly doped sample, for 1 mol. % of Yb_2O_3 the time constant for the $\ ^2F_{5/2} \rightarrow \ ^2F_{7/2}$ transition of Yb^{3+} is $(0.78 \pm 0.04) \text{ ms}$ and decreases to $(0.16 \pm 0.01) \text{ ms}$ in the sample codoped with 0.01 mol. % of Er_2O_3 (Fig. 5). Therefore the energy transfer efficiency is given by $\eta = 1 - \tau_f/\tau = 80\%$, where $\tau_f = (0.16 \pm 0.01) \text{ ms}$ and $\tau = (0.78 \pm 0.04) \text{ ms}$.

The nonradiative transition rate of the codoped lead fluoroborate glass can be evaluated from the radiative transition rate calculated above and the measured fluorescence lifetime of Er^{3+} . The measured decay rate of the fluorescence ($A_{\text{meas}} = 1/\tau_f = 769.2 \text{ s}^{-1}$) from the excited-state energy level of a rare earth is given by $A_{\text{meas}} = A_R + A_{\text{NR}}$, where A_R is the radiative transition rate calculated previously from the Judd–Ofelt analysis [340.6 s^{-1} ; Eq. (3)] and A_{NR} is the nonradiative transition rate, expressed by $A_{\text{NR}} = 1/\tau_f - 1/\tau_R = 428.6 \text{ s}^{-1}$ (where $\tau_R = 2.94 \text{ ms}$ is the calculated radiative lifetime and

Table 1. Fluorescence Lifetimes τ of Singly and Codoped Lead Fluoroborate Glasses

Dopant		τ_f ($\pm 5\%$; ms)	Transition
Er_2O_3 (mol. %)	Yb_2O_3 (mol. %)		
0.20	-	1.30	$\ ^4I_{13/2} \rightarrow \ ^4I_{15/2}$
0.50	-	1.10	$\ ^4I_{13/2} \rightarrow \ ^4I_{15/2}$
1.00	-	0.91	$\ ^4I_{13/2} \rightarrow \ ^4I_{15/2}$
2.00	-	0.80	$\ ^4I_{13/2} \rightarrow \ ^4I_{15/2}$
0.01	1.00	1.30	$\ ^4I_{13/2} \rightarrow \ ^4I_{15/2}$
0.01	1.00	0.16	$\ ^2F_{5/2} \rightarrow \ ^2F_{7/2}$
	1.00	0.78	$\ ^2F_{5/2} \rightarrow \ ^2F_{7/2}$

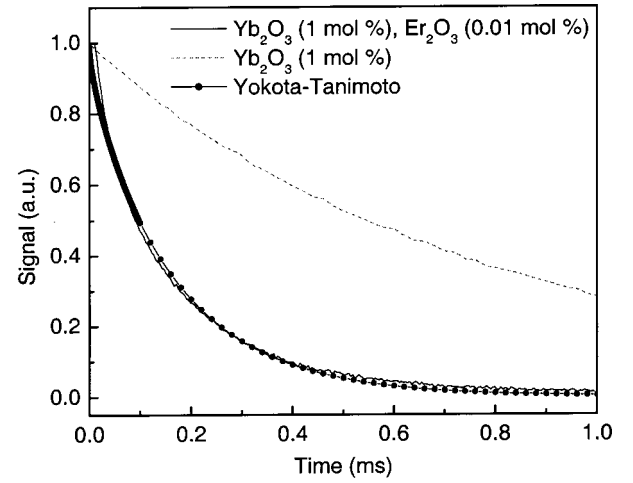


Fig. 6. Time evolution of the Yb^{3+} fluorescence in lead fluoroborate glasses singly doped with Yb_2O_3 and codoped with Yb_2O_3 and Er_2O_3 . The evolution was also fitted by use of the Yokota–Tanimoto expression.

$\tau_f = 1.3 \text{ ms}$ is the measured fluorescence lifetime of Er^{3+} for the codoped sample). The quantum efficiency is governed by the nonradiative rate and is given by $\varepsilon = \tau_f/\tau_R = 44\%$.

The experimentally measured evolution of the Yb^{3+} fluorescence lifetime in the codoped sample was also fitted (Fig. 6) by use of the Yokota–Tanimoto expression^{10,13}

$$N(t) = \exp \left[-\frac{t}{\tau} - bt^{1/2} \left(\frac{1 + 10.87x + 15.50x^2}{1 + 8.743x} \right)^{3/4} \right], \quad (5)$$

where $x = DR_0^{-2}\tau^{1/3}t^{2/3}$, $D = KC_{\text{Yb}}^{4/3}$, $b = 4/3\pi^{3/2} \times C_A R_0^3 \tau^{-1/2}$, and $W_{\text{DA}} = C_{\text{DA}}/R^6$, with $C_{\text{DA}} = R_0^6/\tau$.

In Eq. (5), τ is the experimentally measured Yb^{3+} lifetime in the singly doped glass, D is the Yb^{3+} diffusion constant that is due to the excitation energy migration, R is the donor–acceptor distance, R_0 is the critical radius of the Yb^{3+} – Er^{3+} dipole–dipole interaction, and C_A and C_{Yb} are the Er^{3+} and Yb^{3+} concentrations, respectively; W_{DA} is the transfer probability from the donor to the acceptor, and C_{DA} is the donor–acceptor energy transfer parameter. This model considers the effects of diffusion-limited energy transfer between rare-earth ions; the fit to the experimental decay of the donor ion permits determination of the diffusion constant [$D = (1.6 \pm 0.2) \times 10^{-10} \text{ cm}^2$] and the critical radius [$R_0 = (18 \pm 1) \times 10^{-8} \text{ cm}$]. We remark that these values are similar to those of niobium alkali tellurite glasses codoped with Tm^{3+} and Ho^{3+} . However, in that case the energy transfer efficiency is 50.0%.¹⁴

4. DISCUSSION

The Yb^{3+} absorption cross section in singly doped lead fluoroborate glass is high [$(2.80 \pm 0.19) 10^{-20} \text{ cm}^2$], and its long fluorescence lifetime of $(0.78 \pm 0.04) \text{ ms}$ decreases to $(0.16 \pm 0.01) \text{ ms}$ in the presence of Er^{3+} ,

showing an energy transfer from Yb^{3+} to Er^{3+} with efficiency of 80%. This energy transfer can be also observed by comparison of the emission of the singly doped sample (only Yb^{3+}) with the codoped sample (Fig. 2).

The Er^{3+} emission, related to the ${}^4I_{13/2} \rightarrow {}^4I_{15/2}$ transition, increases with the erbium concentration. However, in the presence of Yb^{3+} (Fig. 4) it is significantly enhanced, even when the concentration of Er_2O_3 is decreased by a factor of 100, showing that energy transfer occurs from Yb^{3+} to Er^{3+} . To obtain a fluorescence signal of such magnitude in the singly doped samples it would be necessary to increase the concentration of Er_2O_3 significantly. However, the measurements show a quenching of the luminescence for concentrations higher than 2 mol. % of Er_2O_3 . Also, the results obtained show that the 1543-nm emission of the singly doped Er^{3+} sample does not have the same properties as those observed for the codoped sample. These are a fluorescence lifetime of (1.30 ± 0.07) ms and high fluorescence emission.

The emission band at 1500 nm is larger (72.4 nm) than in other glass hosts (phosphate glasses have emission bandwidths of ~ 50 nm) used for lasers in the third optical communication window and is therefore of interest for wavelength-division multiplexing.¹⁵

We calculated the Judd–Ofelt parameters and used them to determine the emission cross-section spectrum of Er^{3+} for the codoped sample, whose peak value of $(0.73 \pm 0.06) \times 10^{-20}$ cm² at 1543 nm is comparable to those of the following Yb–Er phosphate laser glasses used at 1500 nm: IOG-1 (0.61×10^{-20} cm²),¹⁶ Qe-7 from Kigre, Incorporated (0.8×10^{-20} cm²),⁹ and $\text{LaLiP}_4\text{O}_{12}$ (0.80×10^{-20} cm²).² The experimentally measured decay curve of the codoped Yb^{3+} sample could be fitted by the Yokota–Tanimoto expression, as can be seen from Fig. 6. Therefore the Yb^{3+} concentration used in the diffusion-limited model for the energy transfer between Yb^{3+} and Er^{3+} could be applied.

The specific concentration quenching mechanism varies with the rare-earth species but in all cases has a common outcome: As the concentration is increased, it becomes more probable that energy will find its way to nonradiative relaxation paths and will ultimately be dissipated.

In erbium-doped hosts, concentration quenching is caused by resonant energy transfer followed by hydroxyl (OH) quenching,^{17–19} cooperative upconversion,²⁰ or both. The resonant energy is critical for highly doped hosts. Upconversion is most problematic for strong optical pumping. At low pump powers the predominant loss mechanism is associated with the presence of OH.²¹ The vibration frequency of the OH group in vitreous systems falls within the range 2800–3700 cm⁻¹,²² which is much larger than the maximum phonon energy of a typical glass host. The ${}^4I_{13/2} \rightarrow {}^4I_{15/2}$ transition of Er^{3+} can be bridged by only two OH phonons, making the occurrence of this process much more probable than multiphonon decay by the glass matrix alone.

In our case the concentration of Er_2O_3 as well as the pump power (7.5 W) is low. Therefore, based on the discussion above, a quantum efficiency of $\sim 50\%$ may be attributed to nonradiative decay related to the energy transfer to OH.

5. CONCLUSIONS

Energy transfer with an efficiency of 80% was measured in a new lead fluoroborate glass ($\text{PbO-PbF}_2\text{-B}_2\text{O}_3$) codoped with Yb_2O_3 (1 mol. %) and Er_2O_3 (0.01 mol. %). In terms of efficiency, the best concentration of Er_2O_3 within the lead fluoroborate glass is 100 times smaller than the concentration of Yb_2O_3 . We remark on the large emission band (72.4 nm) measured at 1543 nm. The peak emission cross section for this ${}^4I_{13/2} \rightarrow {}^4I_{15/2}$ transition is $(0.73 \pm 0.06) \times 10^{-20}$ cm², and the fluorescence lifetime is (1.30 ± 0.07) ms. The samples presented good mechanical resistance for diode laser pumping (7.5 W of diode output power). This is, to our knowledge, the first report of lead fluoroborate glass codoped with Er^{3+} and Yb^{3+} . The results obtained show that this new material has good prospects for laser action near 1543 nm.

ACKNOWLEDGMENT

The authors acknowledge financial support from the Fundação, de Amparo a Pesquisa do Estado de São Paulo.

L. R. P. Kassab's e-mail address is kassablml@osite.com.br.

REFERENCES

1. E. Snitzer and R. Woodcock, "Yb³⁺–Er³⁺ glass laser (room temperature 3-level laser energy transfer from Yb³⁺ to Er³⁺)," *Appl. Phys. Lett.* **6**, 45–49 (1965).
2. A. F. Obaton, C. Parent, G. Le Flem, P. Thony, A. Brenier, and G. Boulon, "Yb–Er codoped LaLiPO_4 glass: a new eye-safe at 1535 nm," *J. Alloys Compd.* **300**, 123–130 (2000).
3. M. Okayasu, T. Takeshita, M. Yamada, O. Kogure, M. Horiguchi, M. Fukuda, A. Kozen, K. Oe, and S. Uehara, "High-power 0.98 μm GaInAs strained quantum well lasers for Er³⁺ doped fiber amplifier," *Electron. Lett.* **25**, 1563–1565 (1989).
4. R. J. Mears, L. Reekie, I. M. Jauncey, and D. N. Payne, "Low noise erbium doped fiber amplifier operating at 1.54 μm ," *Electron. Lett.* **23**, 1026–1027 (1987).
5. S. Taccheo, G. Sorbello, P. Laporta, and C. Svelto, "Analysis of long-term absolute frequency stabilization of a bulk 1.5-m erbium microlaser to a grid of nine different wavelengths," *Electron. Lett.* **34**, 81–82 (1998).
6. J. Nees, S. Biswal, F. Druon, J. Faure, M. Nantel, G. A. Mourou, A. Nishimura, H. Takuma, J. Itatani, J. Christophe Chanteloup, and C. Honninger, "Ensuring compactness, reliability, and scalability for the next generation of high field lasers," *IEEE J. Quantum Electron.* **4**, 376–384 (1998).
7. L. R. P. Kassab, S. H. Tatum, A. S. Morais, L. C. Courrol, N. U. Wetter, and V. L. R. Salvador, "Spectroscopic properties of lead fluoroborate glasses doped with ytterbium," *Opt. Express* **8**, 585–589 (2001), <http://www.opticsexpress.org>.
8. L. R. P. Kassab, L. C. Courrol, N. U. Wetter, L. Gomes, V. L. R. Salvador, and A. S. Morais, "Lead fluoroborate glasses doped with ytterbium," *J. Alloys Compd.* (to be published).
9. P. Laporta, S. Taccheo, S. Longhi, O. Svelto, and C. Svelto, "Erbium–ytterbium microlasers: optical properties and lasing characteristics," *Opt. Mater.* **11**, 269–288 (1999).
10. B. Di Bartolo, *Optical Properties of Ions in Solids* (Plenum, New York, 1975), pp. 66–325.
11. W. T. Carnall, P. R. Fields, and K. Rajnak, "Spectral inten

- sities of the trivalent lanthanides and actinides in solution. II. Pm^{3+} , Sm^{3+} , Eu^{3+} , Gd^{3+} , Tb^{3+} , Dy^{3+} , and Ho^{3+} ," *J. Chem. Phys.* **49**, 4412–4423 (1968).
12. M. J. Weber, "Probabilities for radiative and nonradiative decay of Er^{3+} in LaF_3 ," *Phys. Rev.* **157**, 157–272 (1967).
 13. M. Yokota and O. Tanimoto, "Effects of diffusion on energy transfer by resonance," *J. Phys. Soc. Jpn.* **22**, 779–784 (1967).
 14. L. C. Courrol, L. V. G. Tarelho, L. Gomes, N. D. Vieira, Jr., F. C. Cassanjes, and Y. Messaddeq, "Time dependence and energy transfer mechanism in Tm^{3+} , Ho^{3+} and Tm^{3+} - Ho^{3+} co-doped alkali niobium tellurite glasses sensitized by Yb^{3+} ," *J. Non-Cryst. Solids* **284**, 217–222 (2001).
 15. S. Taccheo, P. Laporta, S. Longhi, O. Svelto, and C. Svelto, "Diode pumped bulk erbium ytterbium," *Appl. Phys. B* **63**, 425–436 (1996).
 16. D. L. Veasey, D. S. Funk, P. M. Peters, N. A. Stanford, G. E. Obarski, N. Fontaine, M. Young, A. P. Peskin, W.-Chih Liu, S. N. Houde-Walter, and J. S. Haydenc, "Yb/Er-codoped and Yb-doped waveguide lasers in phosphate glasses," *J. Non-Cryst. Solids* **263**, 369–381 (2000).
 17. Y. Yan, A. J. Faber, and H. de Waal, "Luminescence quenching by OH groups in highly Er-doped phosphate glasses," *J. Non-Cryst. Solids* **181**, 283–290 (1995).
 18. H. Ebendorff-Heidepriem, W. Seeber, and D. Ehrt, "Spectroscopic properties of Nd^{3+} ions in phosphate glasses," *J. Non-Cryst. Solids* **183**, 191–200 (1995).
 19. E. Snoeks, P. G. Kik, and A. Polman, "Concentration quenching in erbium implanted alkali silicate glasses," *Opt. Mater.* **5**, 159–167 (1996).
 20. M. P. Hehle, N. J. Cockroft, T. R. Gosnell, A. J. Bruce, G. Nykolak, and J. Schmulovich, "Uniform upconversion in high concentration Er^{3+} -doped soda lime silicate and aluminosilicate glasses," *Opt. Lett.* **22**, 772–774 (1997).
 21. S. N. Houde-Walter, P. M. Peers, J. F. Stebbins, and Q. Zeng, "Hydroxyl-contents and hydroxyl related concentration quenching in erbium-doped aluminophosphate, aluminosilicate and fluorosilicate glasses," *J. Non-Cryst. Solids* **286**, 118–131 (2001).
 22. L. Zhang, H. Hu, and F. Lin, "Emission properties of highly doped Er fluoroaluminate glass," *Mater. Lett.* **47**, 189–193 (2001).